Standard Radiometers and Targets for Microwave Remote Sensing*

J. Randa, A.E. Cox, D.K. Walker, M. Francis, J. Guerrieri, and K. MacReynolds
Electromagnetics Division
National Institute of Standards and Technology Boulder, CO 80305, U.S.A.
randa@boulder.nist.gov

***Abstract*—We describe the NIST effort to develop brightness-temperature standards for microwave and millimeter-wave frequencies. Results of preliminary measurements at 26 GHz are presented.**

Keywords-brightness temperature, microwave radiometry, radiometer calibration, remote sensing, standards

I. Introduction

The Electromagnetics Division of the U.S. National Institute of Standards and Technology (NIST) is engaged in an effort to improve calibration methods and tools for microwave remote-sensing radiometry. A principal component of this effort is the development of standard radiometers and standard calibration targets. NIST already has a set of microwave radiometers that measure noise temperature at a coaxial or waveguide reference plane. These will be converted (reversibly) to standard remote-sensing radiometers by the simple expedient of connecting a well characterized antenna to the radiometer input, where one would "normally" connect a noise source whose noise temperature is to be measured. Because these radiometers are calibrated using two primary noise standards, one at ambient temperature and one at cryogenic (liquid nitrogen) temperature, this will provide a link from microwave remote-sensing measurements to the fundamental noise standards maintained by NIST, and will constitute a physical standard for microwave brightness temperature. The standard calibration targets will be developed independently and will be used both as a check of the standard radiometers and as portable artifacts for calibration of radiometers at clients' facilities, in much the same manner as is done at optical frequencies by the NIST Optical Technology Division [1].

A physical standard for microwave brightness temperature offers a number of benefits, all derived from the existence of a stable, common point of reference to which different measurements by different instruments at different times can be compared. Thus, for example, measurements from two different satellites could be meaningfully compared and reconciled if both were traceable to fundamental standards. The standard will also provide a stable reference point that would allow comparisons of data from satellites flown years or decades apart, a critical issue for studying long-term phenomena such as climate change.

Section II below outlines the theoretical framework for the standard radiometers and a simple estimate of the achievable uncertainty. Section III describes and presents results from preliminary measurements. In Section IV we discuss methods for comparing to the brightness-temperature standard and summarize the work.

II. Theoretical Framework

A. Theoretical Framework

The NIST microwave radiometers measure noise temperature at a coaxial or waveguide reference plane. These radiometers are calibrated using two primary noise standards, one at ambient temperature, the other at cryogenic (liquid nitrogen) temperature. Therefore, in order to link microwave remote-sensing measurements to the primary noise standards, we need to relate the measurand in a remote sensing radiometer to the noise temperature at the output of the antenna, plane x in Fig. 1. That relationship will enable us to measure the brightness temperature of a calibration target, thereby providing an independent confirmation of the nominal value of its brightness temperature, and link that value to fundamental noise standards. The development below follows that in [2]; an earlier version of the current work, with full details of the development, can be found in [3]. Far-field conditions are assumed throughout the theoretical development.

Radiometers used in microwave remote sensing measure the radiated power incident on the radiometer's antenna, but the results are usually expressed in terms of a brightness temperature which is defined in terms of the spectral brightness. The brightness $B(\theta,\phi)$ is the power per unit area and solid angle incident on (or emitted from) a surface, and the spectral brightness $B_f(\theta,\varphi)$ is the brightness per unit frequency.

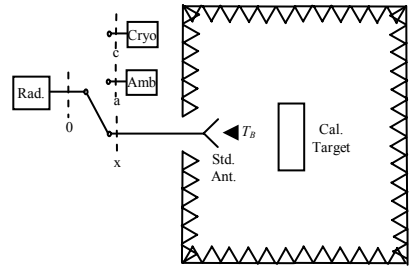

Figure 1. Standard-radiometer configuration.

* U.S. government work; not protected by U.S. copyright.
Supported in part by the NOAA/NESDIS/Integrated Program Office.

US Government work not protected by US Copyright

We define the brightness temperature $T_B(\theta, \varphi)$ by

$$T_B(\theta,\phi) \equiv \frac{\lambda^2 B_f(\theta,\phi)}{2k} \ , \qquad (1)$$

where λ is the wavelength, and k is Boltzmann's constant. (This differs from the conventional definition [2,3], in which (1) holds only in the Rayleigh-Jeans approximation, $kT << hf$.) In terms of the incident brightness temperature, the power received by an antenna can be written as

$$P = kT_{A,in}\Delta f \ , \qquad (2)$$

where $T_{A,in}$ is the input antenna temperature (*i.e.*, at the antenna aperture), defined as

$$T_{A,in} \equiv \frac{A_{eff}}{\lambda^2}\int_{4\pi} T_B(\theta,\phi)F_n(\theta,\phi)d\Omega \ , \qquad (3)$$

where A_{eff} is the (maximum) effective aperture of the antenna, $T_B(\theta,\varphi)$ is the brightness temperature incident on the antenna, and $F_n(\theta,\varphi)$ is the normalized antenna pattern. The integral in (3) covers the full 4π solid angle, whereas our interest is in the component of $T_{A,in}$ due to the target under test. We therefore break $T_{A,in}$ into two parts, one containing the integral over the solid angle subtended by the target of interest, and the other containing the rest. In common remote-sensing applications, this integral is taken over the main beam, so that the main beam *defines* the target or scene. For our application, we wish to separate the calibration-target component from everything else. Thus, the target may intercept more or less of the pattern than just the main beam. We also define the antenna-target efficiency η_{AT} as the fraction of the antenna pattern subtended by the target,

$$\eta_{AT} \equiv \frac{\int_{\text{target}} F_n(\theta,\phi)d\Omega}{\Omega_p} \ , \qquad (4)$$

where $\Omega_p = \int_{4\pi} F_n(\theta,\phi)d\Omega$. Then $T_{A,in}$ can be written as

$$T_{A,in} = \eta_{AT}\overline{T_T} + (1-\eta_{AT})\overline{T_{BG}} \ , \qquad (5)$$

where

$$\overline{T_T} = \frac{\int_{\text{target}} T_B(\theta,\phi)F_n(\theta,\phi)d\Omega}{\int_{\text{target}} F_n(\theta,\phi)d\Omega}$$
$$\overline{T_{BG}} = \frac{\int_{\text{other}} T_B(\theta,\phi)F_n(\theta,\phi)d\Omega}{\int_{\text{other}} F_n(\theta,\phi)d\Omega} \ . \qquad (6)$$

The input antenna temperature $T_{A,in}$ is related to the noise temperature at the antenna waveguide or coaxial output by $T_{A,out} = \alpha T_{A,in} + (1-\alpha)T_a$, where α is the available power ratio between the two planes (approximately equal to the inverse of the loss factor L), $\overline{T_{BG}}$ is the effective background brightness temperature, and T_a is the noise temperature corresponding to the physical temperature of the antenna. Using (5) we can then write

$$\overline{T_T} = \frac{1}{\alpha\eta_{AT}}T_{A,out} - \frac{(1-\eta_{AT})}{\eta_{AT}}\overline{T_{BG}} - \frac{(1-\alpha)}{\alpha\eta_{AT}}T_a \ . \qquad (7)$$

To reduce the effect of $\overline{T_{BG}}$ in (7), we need to control the environment in which the standard radiometer operates. We intend to use a shielded enclosure with absorptive walls, maintained at room temperature, which will also be the temperature of the antenna, T_a. Then $\overline{T_{BG}} = T_a$, and (7) becomes

$$\overline{T_T} = T_a + \frac{1}{\alpha\eta_{AT}}\left(T_{A,out} - T_a\right). \qquad (8)$$

Equation (8) is the desired result for our standard-radiometer measurements. It expresses the average incident brightness temperature received from the target $\overline{T_T}$ in terms of $T_{A,out}$, α, η_{AT}, and T_a. Note that $\overline{T_T}$ will contain contributions not just from target emission, but also from background radiation scattered by the target; these quantities will be dependent upon the target emissivity. In (8) $T_{A,out}$ is the noise temperature at the output of the antenna, measured by the radiometer; α is the available power ratio between the antenna aperture and its output, approximately equal to $1/L$; η_{AT} is the antenna-target efficiency, defined in (4) and determined from the normalized antenna pattern; and T_a is the noise temperature corresponding to the physical temperature of the antenna and the enclosure.

B. *Estimate of Achievable Uncertainty*

We expect to be able to control $\overline{T_{BG}}$ and T_a to within about 0.2 K. Over the 200 K – 300 K range, $T_{A,out}$ can be measured with a standard uncertainty of about 0.3 K up to about 26 GHz. Assuming we use a simple antenna, such as a standard-gain horn, ohmic losses are best determined by calculation, using any of a number of software packages. For common, commercial standard-gain horns the ohmic losses are less than 0.03 dB for the worst-case conductivity. The uncertainty in the electrical conductivity is the major uncertainty in determining the ohmic losses, and it will lead to a fractional uncertainty of about 0.5 % in α. The antenna-target efficiency η_{AT} can be determined from a measurement of the antenna pattern. For the antenna pattern measurements of the next section, the uncertainty in η_{AT} due to the uncertainty in the antenna pattern is approximately 0.003. If the uncertainty in the target solid angle is negligible, the uncertainty in η_{AT} will then be ~0.003, and we should be able to achieve a standard uncertainty in $\overline{T_T}$ of about 0.3 K to 0.8 K for $\overline{T_T}$ between 200 K and 300 K. For higher temperatures, the uncertainty in $\overline{T_T}$ will be larger due to an increase in the uncertainty in the measurement of $T_{A,out}$.

US Government work not protected by US Copyright

III. Measurements

A. Antenna Pattern

We measured a standard-gain horn (with nominal gain of 25 dB) on the NIST spherical probe pattern range. The forward hemisphere (θ ranges from -90° to 90°) pattern was determined at 2 degree increments in θ and 5 degree increments in φ. The φ=0° pattern is shown in Fig. 2. The pattern was integrated over the angle subtended by the standard target and compared to the total integrated power. The beam efficiency was calculated for several distances between the horn and the target. The efficiency for the closest position of 50 cm was found to be 0.98. The uncertainty in the calculation of this efficiency is dominated by uncertainties in the target aperture dimensions. In the present work, near-field effects were not considered and may apply at our closest measurement distances.

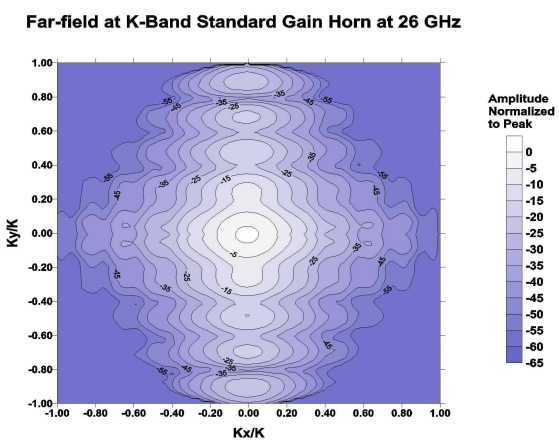

Figure 2. Far-field antenna pattern for standard gain horn at 26 GHz.

B. Standard-Radiometer Setup

Several measurements of $T_{A,out}$ were made in the NIST anechoic chamber while viewing a calibration target. The characterized standard-gain horn was connected to the WR-42 standard waveguide radiometer and pointed at the center of a calibration target mounted on a positioning system inside a nominally temperature-controlled chamber. The positioning system consists of a rail-mounted computer-controlled stage shielded by absorber. The target position was moved relative to the radiometer by stepping the stage position back from 50 cm to approximately 5 m. Radiometer measurements were made for different distances between the horn and target and for target temperatures of ambient and approximately 350 K. The target temperature and chamber temperature were monitored and recorded throughout the experiment.

The standard radiometer employs an integrated six-port reflectometer to measure relevant reflection coefficients [4]. Each view of the antenna port (and thus the calibration target) is bracketed by radiometer views of the two primary noise standards (cryogenic and ambient). Radiometer measurements were made at 18, 22, and 26 GHz for each distance. Results are presented for 26 GHz.

The results presented used a hot calibration target from the NOAA Ground-Based Scanning Radiometer (GSR) [5]. This custom target has an aperture of approximately 67 x 43 cm and consists of canted foam pyramids lining the interior of a tent-shaped aluminum frame. Heating elements behind the foam elevate the target temperature and fans circulate heated air to reduce thermal gradients. There are 16 temperature sensors monitoring the temperature of the target, and a closed-loop controller is used to heat and monitor the target performance. The target, heaters, fans, and temperature sensors are housed in a polystyrene enclosure that serves to thermally isolate the target from the surrounding environment.

C. Standard-Radiometer Results

Fig. 3 shows a plot of $\overline{T_T}$ obtained from the radiometer measurements at 26 GHz for different distances from the antenna to the target. It also shows the values for T_B calculated from the target temperature, background temperature, and two emissivity values.

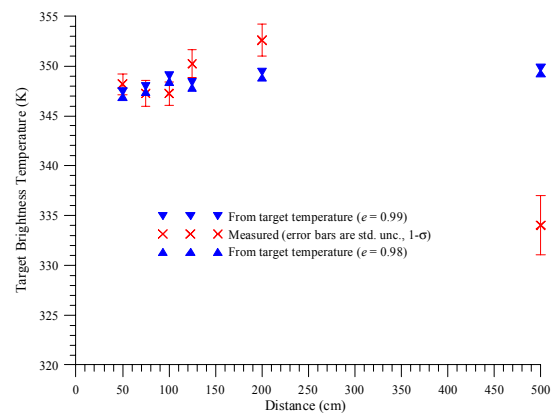

Figure 3. Brightness temperature of a calibration target at 26 GHz.

The uncertainties in the radiometer measurements vary with distance, and for these preliminary results range from 1 – 3 K. The uncertainties are dominated by the uncertainty in the target dimensions and if this uncertainty is removed, they range from 0.7 – 2.3 K depending on distance. These uncertainties can be further reduced through careful control of experimental conditions, and we expect to reduce them below 1 K even for target temperatures around 350 K. The difference between the brightness temperature, as determined by the radiometer, versus that calculated from the target temperature sensors, agree to within a few kelvins for most of the target positions; this difference is not consistent throughout the experiment and increases with the distance to the target. There are several possible reasons for this discrepancy. Since the target aperture was not visible during alignment of the target to the standard gain horn, its exact dimensions and position were not known. These dimensions factor in to the calculation of η_{AT}. The axis of the viewing antenna may not have been aligned with the motion of the movable stage, and during the experiment, some variations in chamber temperature occurred that were greater than the

US Government work not protected by US Copyright

desired 0.2 K. During measurements of the heated target, the target temperature was drifting upwards as it had not yet reached thermal equilibrium. Also, the emissivity of the target is not exactly known and was derived from knowledge of the target materials and similar targets that have been validated in the field. These are all important factors to consider in the development of a standard calibration target.

IV. Discussion and Summary

A. Comparison and Standard Targets

The standard radiometer(s) discussed above will constitute a standard for brightness temperature, linking measurements of it to primary noise standards. For it to be useful, however, there must be a means for others to compare to this standard. One way would be for outside parties to send their calibration targets to NIST, where the targets could be measured by the standard radiometers. Because the standard radiometers will not be used in a thermal-vacuum (TV) chamber, such a comparison would be done at atmospheric pressure. It would also be very useful for NIST to have a transportable transfer standard, which could be measured by the customer's radiometer at the customer's facility. For this purpose, we plan to develop a standard calibration target, in addition to the standard radiometers. Its temperature will be monitored by several thermistors, so that it will constitute a brightness-temperature standard in its own right, but it also will be measured by the standard radiometers, thereby providing a check of both the standard target and the radiometers. This standard calibration target will be designed for use in either ambient or TV chambers, so that it can be used in the same facilities that are used for testing of a customer's radiometer and its calibration targets. An integral part of the development and design of the NIST standard target will be the development of methods for testing and characterizing such targets. In particular, we will attempt to develop test methods for detecting thermal gradients within the target (infrared imaging) and for measuring reflectivity or emissivity of the target.

Assuming both standard radiometers and a transportable standard target are developed, there will be a number of strategies available for comparing to a NIST brightness-temperature standard. In the NIST chamber, a customer's calibration target could be measured directly with a NIST standard radiometer, thereby linking its brightness temperature to primary noise standards (under ambient conditions). A customer's radiometer (within size limitations) could also be measured in the NIST chamber and compared directly to the NIST standard radiometer by measuring the same target with both radiometers. The standard target could also be measured at a customer's facility, either under ambient conditions or in a TV chamber. The performance of the NIST standard target in the NIST ambient chamber could be compared with that in a TV chamber if a portable radiometer was available. The standard target could then be measured by the same radiometer in both the ambient chamber and in a TV chamber. It would also be measured with the NIST standard radiometer in the ambient chamber. This would provide a link of the portable radiometer to the NIST standard radiometer and would also provide a measure of the different behavior of the standard target under ambient and TV conditions.

B. Summary

We plan to develop standards for microwave brightness temperature for the frequency range 18 – 65 GHz, starting with the WR-42 (18 – 26.5 GHz) band. This will be done by connecting characterized antennas to the measurement ports of existing NIST waveguide radiometers, which are calibrated against primary noise standards. Thus the brightness-temperature standard will be tied to the primary noise standards. A chamber will be constructed to provide a controlled environment for using these radiometers at ambient temperature and pressure. At the lowest frequencies, we anticipate a standard uncertainty of about 0.3 K to 0.8 K in the brightness temperature for temperatures in the 200 K – 300 K range. Results of preliminary measurements with such a converted radiometer at 26 GHz were presented. The results are in reasonable agreement with the nominal brightness temperature of the calibration target that was measured, but the uncertainties are larger than anticipated. Uncertainties can be reduced through modifications in the experimental method. Future work includes measurement of a different calibration target and development of methods to better determine target emissivity. In parallel, we plan to develop a portable standard calibration target, which will be suitable for use in a TV environment. The portable standard calibration target will be cross-checked with the standard radiometers. The standards will enable the measurement of customers' radiometers or targets at NIST at ambient temperature and pressure or measurement of the NIST standard target at a customer's facility under either ambient or thermal-vacuum conditions.

Acknowledgment

We thank Al Gasiewski and Marian Klein of the NOAA Environmental Technology Laboratory for use of the GSR hot calibration target. We thank Rob Billinger and Jeff Bridges of NIST for measurement support.

References

[1] J.P. Rice and B.C. Johnson, "NIST activities in support of space-based radiometric remote sensing," Proc. SPIE, Vol. 4450, pp. 108 – 126, 2001.

[2] F. Ulaby, R. Moore, and A. Fung, *Microwave Remote Sensing: Fundamentals and Radiometry, Vol. 1*, Norwood, MA, Artech House, 1981.

[3] J. Randa, "Traceability for microwave remote-sensing radiometry," NIST Interagency Report, NISTIR 6631, June 2004.

[4] J. Randa, L.A. Terrell, "Noise-Temperature Measurement System for the WR-28 Band," NIST Tech. Note, TN1395, August 1997.

[5] NOAA Environmental Technology Laboratory, Ground-Based Scanning Radiometer, http://www.etl.noaa.gov/technology/gsr/

US Government work not protected by US Copyright

IGARSS 2004 Conference Digest
Paper 2TU_30_10

2004 IEEE International Geoscience and Remote Sensing Symposium
20 – 24 September, 2004
Anchorage, Alaska